

Enhanced output entanglement with reservoir engineering

Xiao-Bo Yan*

*College of Electronic Science, Northeast Petroleum University, Daqing 163318, China
and Institute of Theoretical Physics, Chinese Academy of Sciences, Beijing 100190, China*

(Received 10 July 2017; published 13 November 2017)

We study the output entanglement in a three-mode optomechanical system via reservoir engineering by shifting the center frequency of filter function away from resonant frequency. We find the bandwidth of the filter function can suppress the entanglement in the vicinity of resonant frequency of the system, while the entanglement will become strong if the center frequency departs from the resonant frequency. We obtain the approximate analytical expressions of the output entanglement, from which we give the optimal center frequency at which the entanglement takes the maximum. Furthermore, we study the effects of time delay between the two output fields on the output entanglement, and obtain the optimal time delay for the case of large filter bandwidth.

DOI: [10.1103/PhysRevA.96.053831](https://doi.org/10.1103/PhysRevA.96.053831)**I. INTRODUCTION**

Cavity optomechanics [1] exploring the interaction between macroscopic mechanical resonators and light fields, has received increasing attention for the potential to detect of tiny mass, force, and displacement [2–5]. The common optomechanical cavity contains one end mirror, being a macroscopic mechanical oscillator or a vibrating membrane [6–11]. In these optomechanical systems, the motion of a mechanical oscillator can be affected by the radiation pressure of a cavity field, and this interaction can generate various quantum phenomena, such as ground-state cooling of mechanical modes [12–17], electromagnetically induced transparency and normal mode splitting [18–22], nonlinear interaction effects [23–26], and quantum state transfer between photons with vastly differing wavelengths [27–30].

Entanglement is the characteristic element of quantum theory because it is responsible for nonlocal correlations between observables and an essential ingredient in most applications in quantum information. For these reasons, there are a number of theoretical and experimental works on entanglement between macroscopic objects such as between atomic ensembles [31,32] and between superconducting qubits [33–36]. Recently, quantum entanglement in cavity optomechanics has received increasing attention for the potential to use the interaction to generate various entanglements between subsystems. For example, quantum entanglement between mechanical resonators [37–40], between different optical modes [41–52], and between mechanical resonators and light modes [53–57] have been studied theoretically and the entanglement between mechanical motion and microwave fields has been demonstrated in a recent experiment [58].

Here, we consider a three-mode optomechanical system in which two cavities are coupled to a common mechanical resonator (see Fig. 1). This setup has been realized in several recent experiments [59–61]. Because in such a system the parametric-amplifier interaction and the beam-splitter interaction can entangle the two intracavity modes, the output cavity modes are also entangled with each other.

In previous works [50,52], the entanglement of two output optical fields with their center frequencies the same as the resonant frequencies of the cavities has been studied. In Ref. [50], the entanglement between the two output fields is enhanced obviously via reservoir engineering [62,63]: cooling the Bogoliubov mode through enhancing mechanical decay results in large entanglement between the two target output fields. But these output entanglements in Refs. [50,52] will be largely limited by the bandwidth of filter function, and the optimal time delay in Ref. [50] between the two output fields is only suitable for the case of little bandwidth of filter function.

In this paper, we first study the effect of filter bandwidth on the output entanglement between the two optical fields without time delay. We find the bandwidth will strongly suppress the output entanglement, specifically as the center frequency of the output fields locates in the vicinity of resonant frequency; whereas, the output entanglement will become strong if the center frequency of output fields departs from the resonant frequency. We will see that the physics behind this phenomenon is the reservoir engineering mechanism because shifting the center frequency can cool the temperature of the system. We obtain all the approximate analytical expressions of the output entanglement in various cases, from which we give the corresponding optimal center frequencies making the entanglement maximum. Finally, we study the effect of the time delay between the two output fields on the output entanglement according to the reservoir engineering mechanism, from which we obtain the approximate analytical expression of the optimal time delay for the case of large filter bandwidth. We believe the results of this paper may be used for reference by experimental and theoretical physicists who work on entanglement or quantum information processing.

The rest of this paper is organized as follows. In Sec. II, we introduce the three-mode optomechanical model with a corresponding equivalent model, and the definition of canonical mode operators of the two output optical fields. In Sec. III, we study the entanglement between the two output optical fields by shifting the center frequency of filter function from resonant frequency, and we study the effects of time delay on the output entanglement. Finally, the conclusions are given in Sec. IV.

*yxb@itp.ac.cn

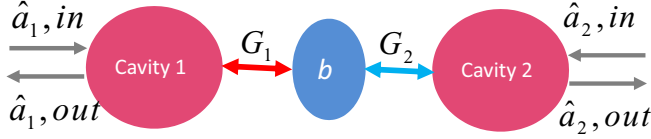


FIG. 1. A three-mode optomechanical system with a mechanical resonator (mode \hat{b}) interacted with two cavities (cavities 1 and 2). Cavity 1 is driven with a red-detuned laser, while cavity 2 is driven with a blue-detuned laser. The entanglement between the output fields of two cavities can be generated.

II. SYSTEM AND AN EQUIVALENT MODEL

We consider a three-mode optomechanical system in which two cavities are coupled to a common mechanical resonator (see Fig. 1).

The standard optomechanical Hamiltonian

$$H = \omega_m \hat{b}^\dagger \hat{b} + \sum_{i=1,2} [\omega_i \hat{a}_i^\dagger \hat{a}_i + g_i (\hat{b}^\dagger + \hat{b}) \hat{a}_i^\dagger \hat{a}_i] \quad (1)$$

governs the system's dynamics, where \hat{a}_i is the annihilation operator for cavity i with frequency ω_i and damping rate κ_i , \hat{b} is the annihilation operator for a mechanics resonator with frequency ω_m and damping rate γ , and g_i is the optomechanical coupling strength. In order to generate the steady entanglement between the two output fields, we drive cavity 1 (2) at the red (blue) sideband with respect to the mechanical resonator: $\omega_{d1} = \omega_1 - \omega_m$ and $\omega_{d2} = \omega_2 + \omega_m$. If we work in a rotating frame with respect to the free Hamiltonian, following the standard linearization procedure, and make the rotating-wave approximation (in this paper, we focus on the resolved-sideband regime $\omega_m \gg \kappa_1, \kappa_2$), then the Hamiltonian of the system can be written as

$$\hat{H}_{\text{int}} = G_1 \hat{b}^\dagger \hat{d}_1 + G_2 \hat{b} \hat{d}_2 + \text{H.c.} \quad (2)$$

Here, $\hat{d}_i = \hat{a}_i - \bar{a}_i$, \bar{a}_i being the classical cavity amplitude. G_i is the effective coupling strength. The combined swapping and entangling interactions in \hat{H}_{int} lead to a net entangling interaction between the two intracavity modes as discussed in [47].

Based on Eq. (2), the dynamics of the system is described by the following quantum Langevin equations for relevant operators of mechanical and optical modes:

$$\begin{aligned} \frac{d}{dt} \hat{b} &= -\frac{\gamma}{2} \hat{b} - i(G_1 \hat{d}_1 + G_2 \hat{d}_2^\dagger) - \sqrt{\gamma} \hat{b}^{\text{in}}, \\ \frac{d}{dt} \hat{d}_1 &= -\frac{\kappa_1}{2} \hat{d}_1 - iG_1 \hat{b} - \sqrt{\kappa_1} \hat{d}_1^{\text{in}}, \\ \frac{d}{dt} \hat{d}_2^\dagger &= -\frac{\kappa_2}{2} \hat{d}_2^\dagger + iG_2 \hat{b} - \sqrt{\kappa_2} \hat{d}_2^{\text{in},\dagger}. \end{aligned} \quad (3)$$

After the linearization, the cavity mode part is about the fluctuations \hat{d}_i , so the coherent drive is no longer in the drive terms of the equations and only contributes to the effective coupling intensity G_i . Here, $\hat{b}^{\text{in}}, \hat{d}_i^{\text{in}}$ are the input noise operators of mechanical resonator and cavity i ($i = 1, 2$), whose correlation functions are $\langle \hat{b}^{\text{in},\dagger}(t) \hat{b}^{\text{in}}(t') \rangle = N_m \delta(t - t')$ and $\langle \hat{d}_i^{\text{in},\dagger}(t) \hat{d}_i^{\text{in}}(t') \rangle = N_i \delta(t - t')$, respectively. N_m and N_i are the average thermal populations of mechanical mode

and cavity i , respectively. In the following discussion, we mainly study the effects of shifting filter center frequency, and the filter bandwidth on the output entanglement, so we assume these average thermal populations are zero (zero temperature). In accordance with the Routh-Hurwitz stability conditions [64], we focus on the regime of strong cooperativities $C_i \equiv 4G_i^2/(\gamma\kappa_i) \gg 1$ and $\kappa_i \gg \gamma$ in this paper; the stability condition of our system can be obtained as $G_1^2/G_2^2 > \max(\kappa_1/\kappa_2, \kappa_2/\kappa_1)$ for $\kappa_1 \neq \kappa_2$, and the system is always stable if $\kappa_1 = \kappa_2$ and $G_2 \leq G_1$ [47,50].

For simplicity, we adopt a rectangle filter with a bandwidth σ centered about the frequency ω to generate the output temporal modes. Then, the canonical mode operators of the two output fields can be described as

$$\hat{D}_i^{\text{out}}[\omega, \sigma, \tau_i] = \frac{1}{\sqrt{\sigma}} \int_{\omega_-}^{\omega_+} d\omega' e^{-i\omega'\tau_i} \hat{d}_i^{\text{out}}(\omega'). \quad (4)$$

Here, $\omega_{\pm} = \omega \pm \frac{\sigma}{2}$, and τ_i is the absolute time at which the wave packet of interest is emitted from cavity i . The frequency-resolved output modes $\hat{d}_i^{\text{out}}(\omega) \equiv \int d\omega' e^{i\omega'\tau_i} \hat{d}_i^{\text{out}}(t)/\sqrt{2\pi}$ are related to the input $\hat{d}_i^{\text{in}}(\omega)$ by scattering matrix $S(\omega)$ (see Appendix A), which can be obtained straightforwardly from the Langevin equations and input-output relations [65]. We use the logarithmic negativity (see Appendix B) [66,67] to quantify the entanglement between the two output cavity modes $\hat{D}_1^{\text{out}}[\omega, \sigma, \tau_1]$ and $\hat{D}_2^{\text{out}}[-\omega, \sigma, \tau_2]$. Without loss of generality, we set $\tau_2 = 0$, and we write $\hat{D}_i^{\text{out}}[\omega, \sigma, \tau_i]$ as \hat{D}_i for simplicity in the following.

It can be proven that our system can be mapped to a two-mode squeezed thermal state [50]

$$\hat{\rho}_{12} = \hat{S}_{12}(R_{12}) [\hat{\rho}_1^{\text{th}}(\bar{n}_1) \otimes \hat{\rho}_2^{\text{th}}(\bar{n}_2)] \hat{S}_{12}^\dagger(R_{12}). \quad (5)$$

Here,

$$\hat{S}_{12}(R_{12}) = \exp[R_{12} \hat{D}_1 \hat{D}_2 - \text{H.c.}] \quad (6)$$

is the two-mode squeeze operator, with R_{12} being the squeezing parameter, and $\hat{\rho}_i^{\text{th}}(\bar{n}_i)$ describes a single-mode thermal state with average population \bar{n}_i . Hence, the output fields are completely characterized just by three parameters: \bar{n}_1, \bar{n}_2 , and R_{12} . The relationship between the two-mode squeezed thermal state and our system can be obtained as follows:

$$\begin{aligned} \bar{n}_1 &= \frac{\langle \hat{D}_1^\dagger \hat{D}_1 \rangle - \langle \hat{D}_2^\dagger \hat{D}_2 \rangle - 1 + \sqrt{A^2 - 4|\langle \hat{D}_1 \hat{D}_2 \rangle|^2}}{2}, \\ \bar{n}_2 &= \frac{\langle \hat{D}_2^\dagger \hat{D}_2 \rangle - \langle \hat{D}_1^\dagger \hat{D}_1 \rangle - 1 + \sqrt{A^2 - 4|\langle \hat{D}_1 \hat{D}_2 \rangle|^2}}{2}, \\ R_{12} &= \frac{1}{2} \text{arctanh} \left(\frac{2|\langle \hat{D}_1 \hat{D}_2 \rangle|}{A} \right). \end{aligned} \quad (7)$$

Here, $\langle \hat{D}_1^\dagger \hat{D}_1 \rangle$, $\langle \hat{D}_2^\dagger \hat{D}_2 \rangle$, and $\langle \hat{D}_1 \hat{D}_2 \rangle$ are the correlators of the output cavity modes, which can be obtained by Langevin equations (3) and input-output relations, and $A = \langle \hat{D}_1^\dagger \hat{D}_1 \rangle + \langle \hat{D}_2^\dagger \hat{D}_2 \rangle + 1$. According to Eqs. (5) and (6), the output entanglement E_n of this two-mode squeezed thermal state (if $E_n \geq 0$) can be simply given by

$$E_n = -\ln \left[n_R - \sqrt{n_R^2 - (1 + 2\bar{n}_1)(1 + 2\bar{n}_2)} \right] \quad (8)$$

with $n_R = (\bar{n}_1 + \bar{n}_2 + 1) \cosh 2R_{12}$. It can be seen from Eq. (8) that the entanglement will increase with the increase of the squeezing parameter R_{12} , whereas it will decrease with the increase of the average populations \bar{n}_1, \bar{n}_2 . In the following, it can be seen that shifting the center frequency of filter function from the resonance can evidently cool the temperature of the system (decrease the average populations \bar{n}_1, \bar{n}_2).

III. CAVITY OUTPUT ENTANGLEMENT

For simplicity, we set equal cavity damping rate $\kappa_1 = \kappa_2 = \kappa$, equal coupling $G_1 = G_2 = G$, and $\gamma \ll \sigma, \kappa, G$ in the following. We discuss the output entanglement on two cases: shifting the filter center frequency ω from the resonant frequency (the resonant frequency is zero in the rotating frame) under the condition of small bandwidth ($\sigma \ll \kappa$) and large bandwidth ($\sigma = \kappa$), respectively.

A. Small bandwidth

In this section we discuss the effects of small bandwidth σ ($\sigma \ll \kappa$) on the entanglement between the two output fields. If we shift the filter center frequency ω to satisfy $0 \leq \omega \leq \frac{\sigma}{2}$ (in the rotating frame), the approximate analytical expression of the output entanglement can be simply written as

$$E_n \approx \frac{\pi \gamma}{2\sigma}. \quad (9)$$

It can be seen from Eq. (9) that the entanglement between output fields is not related to the filter center frequency ω and the coupling strength G . And increasing the mechanical decay rate γ can enhance the output entanglement in the vicinity of resonant frequency $\omega = 0$ just as what the author did in Ref. [50], which is the reservoir engineering mechanism because increasing the mechanical decay rate γ can cool the Bogoliubov mode [50]. If the mechanical damping rate γ satisfies $\gamma \ll \sigma$, the entanglement will almost equal zero. It can also be seen from Eq. (9) that the output entanglement can be largely suppressed by increasing the filter bandwidth σ .

If the center frequency ω satisfies $\frac{\sigma}{2} < \omega < \frac{\kappa}{2}$, and the coupling strength G is weak coupling ($G < \kappa$), the analytical expression of the entanglement can be simplified to

$$E_n \approx -\ln \frac{20G^4\sigma^2 + 3\kappa^2\omega^4}{3\omega^2(64G^4 + \sqrt{2}\kappa^2\omega^2)}. \quad (10)$$

The entanglement is plotted in Fig. 2(a) with parameters $\gamma = 1$, $\sigma = 10$, $\kappa = 10^5$, $G = \kappa/10$. The black solid line is the numerical results according to logarithmic negativity, while the red dashed line is plotted according to the analytical expression, Eq. (10). The entanglement is nonmonotonic with the change of center frequency ω , and will reach a maximum as the optimal center frequency $\omega_{\text{opt}} \approx 6^{1/4}G(\sigma/\kappa)^{1/2}$. The entanglement will appear a peak value at resonant frequency ($\omega = 0$) for the case $\sigma = 0$ [50], but the peak will emerge at some center frequency ω for the case $\sigma \neq 0$. We can give a clear reason for this phenomenon from Fig. 2(b) in which the squeezing parameter R_{12} (red dashed line), the thermal populations \bar{n}_1 (blue dotted line), \bar{n}_2 (black solid line) vs the normalized center frequency ω/σ are plotted. It can be seen from Fig. 2(b) that the two thermal populations \bar{n}_1, \bar{n}_2 are very large (the temperature of the equivalent two-mode squeezing

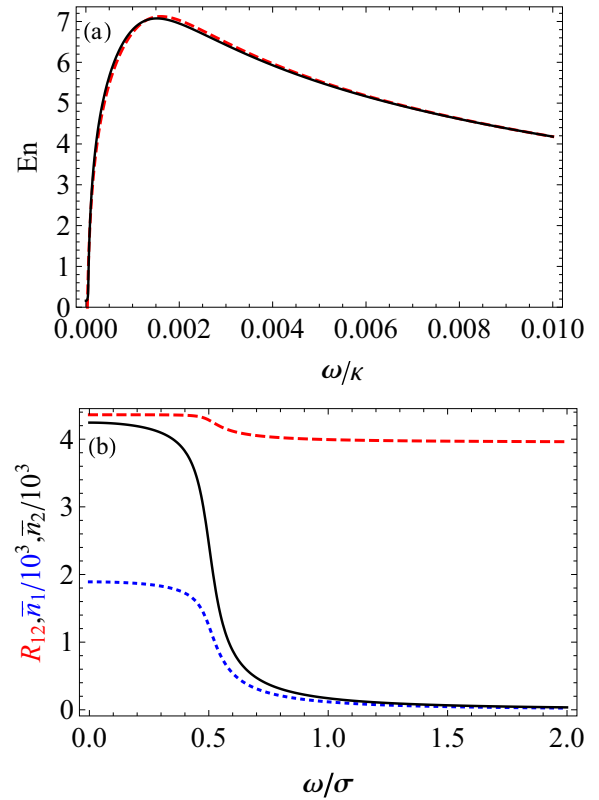


FIG. 2. (a) The entanglement vs the normalized center frequency ω/κ . The black solid line is the numerical results, the red dashed line is plotted according to the analytical expression, Eq. (10). (b) The squeezing parameter R_{12} (red dashed line), the thermal populations $\bar{n}_1/10^3$ (blue dotted line), and $\bar{n}_2/10^3$ (black solid line) vs the normalized center frequency ω/σ . The parameters are $\gamma = 1$, $\sigma = 10$, $\kappa = 10^5$, $G = \kappa/10$.

thermal state is very high) for $\omega < \sigma/2$; then the entanglement is almost zero. But if the center frequency ω becomes larger ($\omega > \sigma/2$), the two thermal populations \bar{n}_1, \bar{n}_2 will decrease rapidly while the squeezing parameter R_{12} decreases very slowly. Hence, the entanglement becomes larger with the increase of center frequency ω until it reaches the highest point. As a result, the optimal center frequency ω_{opt} at which the entanglement reaches a maximum must be greater than $\sigma/2$.

If the coupling strength G is strong coupling ($G > \kappa$), and the filter center frequency ω still satisfies $\frac{\sigma}{2} < \omega < \frac{\kappa}{2}$, the analytical expression of the entanglement can be simplified to

$$E_n \approx -\frac{1}{2} \ln \left[\frac{G^8\sigma^4 + G^4\sigma^2\omega^4\kappa^2 + 2\omega^{10}\kappa^2}{144G^8\omega^4} \right], \quad (11)$$

which reaches a maximum as the optimal center frequency $\omega_{\text{opt}} \approx (G^8\sigma^4/3\kappa^2)^{1/10}$. The entanglement is plotted in Fig. 3(a) with parameters $\gamma = 1$, $\sigma = 10$, $\kappa = 10^5$, $G = 10\kappa$. The black solid line is the numerical results according to logarithmic negativity, while the red dashed line is plotted according to the analytical expression, Eq. (11). It can be seen from Figs. 2 and 3 that the entanglement plotted by the analytical expressions fits the numerical results very well. The thermal populations \bar{n}_1, \bar{n}_2 of strong coupling decrease rapidly

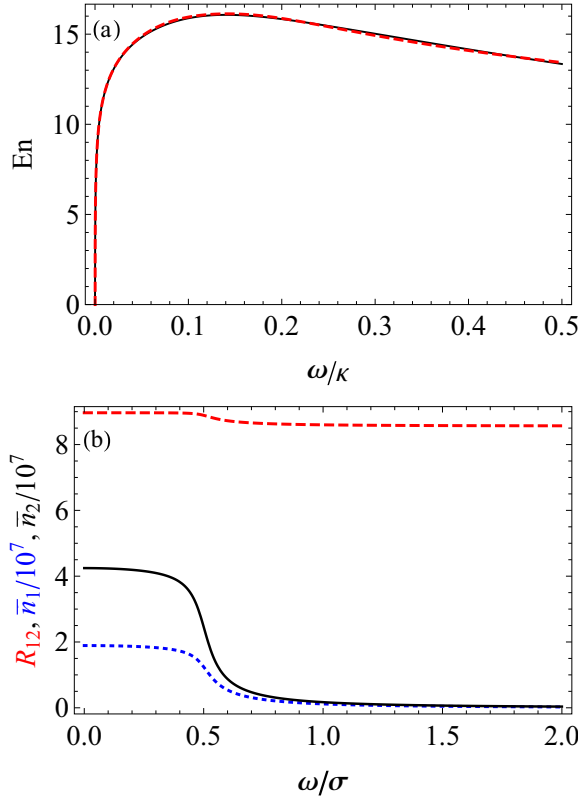


FIG. 3. (a) The entanglement vs the normalized center frequency ω/κ . The black solid line is the numerical results, the red dashed line is plotted according to the analytical expression, Eq. (11). (b) The squeezing parameter R_{12} (red dashed line), the thermal populations $\bar{n}_1/10^7$ (blue dotted line), and $\bar{n}_2/10^7$ (black solid line) vs the normalized center frequency ω/σ . The parameters are $\gamma = 1$, $\sigma = 10$, $\kappa = 10^5$, $G = 10\kappa$.

just like the case of weak coupling as the center frequency $\omega > \sigma/2$. The squeezing parameter R_{12} of strong coupling is larger than that of weak coupling. That is the reason why the entanglement of strong coupling will be larger than that of weak coupling.

According to the above analysis, the optimal center frequency ω_{opt} must be greater than $\sigma/2$, and ω_{opt} will be far away from the resonant frequency ω ($\omega = 0$) if σ is very large. We will discuss the case $\sigma = \kappa$ in the following.

B. Large bandwidth

For $G < \kappa$ and large σ , such as $G = \kappa/10$ and $\sigma = \kappa$, the entanglement will be very small. Hence, in this section, we just discuss the entanglement of strong coupling $G > \kappa$ with the bandwidth $\sigma = \kappa$. Because of $\sigma = \kappa \gg \gamma$, the entanglement will almost be zero when $0 \leq \omega \leq \frac{\kappa}{2}$ according to Eq. (9). The analytical expression of the entanglement can be simplified to

$$E_n \approx \ln \left[\sqrt{2} \left(\frac{3G^4\kappa^2(\omega^2 + \frac{3\kappa^2}{4}) + G^2\kappa^2\omega^4 + \omega^8}{3G^4\kappa^4 + 2G^2\omega^2\kappa^4 + \omega^8} \right) \right] \quad (12)$$

for $\frac{\kappa}{2} \lesssim \omega \lesssim 7\kappa$, and the optimal center frequency $\omega_{\text{opt}} \approx \sqrt{G\kappa}$. In Fig. 4(a), we plot the entanglement vs center

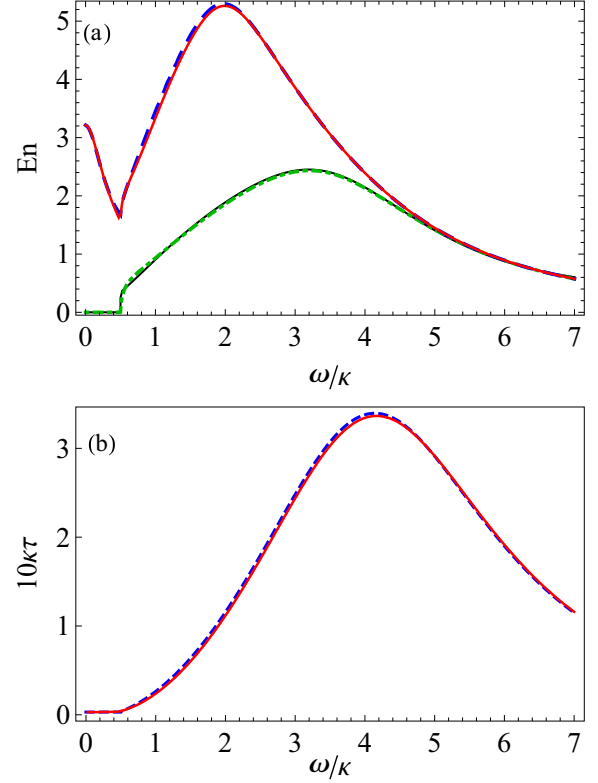


FIG. 4. (a) The entanglement E_n vs the normalized center frequency ω/κ : The red solid line is the entanglement plotted with the optimal time delay, Eq. (14); the blue dashed line is the entanglement plotted with the numerical optimal time delay making the entanglement E_n maximum; the black solid line is the entanglement plotted according to the analytical expression, Eq. (12), without time delay; and the green dashed-dotted line is the entanglement plotted by numerical results according to the logarithmic negativity without time delay. (b) The optimal time delay τ_{opt} (red solid line) according to Eq. (14) and the numerical optimal time delay (blue dashed line). The parameters are $\gamma = 1$, $\sigma = \kappa = 10^5$, $G = 10\kappa$.

frequency ω/κ according to the analytical expression, Eq. (9), Eq. (12) (black solid line), and the numerical results according to the logarithmic negativity (green dashed-dotted line) under the parameters $\gamma = 1$, $\sigma = \kappa = 10^5$, $G = 10\kappa$. It can be seen from Fig. 4(a) that there is still large entanglement even with large bandwidth ($\sigma = \kappa$). This is because shifting the center frequency can effectively cool the two thermal populations \bar{n}_1, \bar{n}_2 via reservoir engineering as discussed above. And the tendencies of the two thermal populations \bar{n}_1, \bar{n}_2 and the squeezing parameter R_{12} are almost the same as the previous cases in Figs. 2(b) and 3(b); we do not discuss them anymore.

As in the above analysis, large bandwidth σ must strongly influence the entanglement of the two output fields. According to the definition of the canonical mode operators \hat{D}_i [see Eq. (4)], the correlator of the output cavity modes $\langle \hat{D}_1 \hat{D}_2 \rangle$ is connected with time delay τ , while the other two correlators $\langle \hat{D}_1^\dagger \hat{D}_1 \rangle$ and $\langle \hat{D}_2^\dagger \hat{D}_2 \rangle$ are not. The expression $\langle \hat{D}_1 \hat{D}_2 \rangle$ can be

written explicitly as

$$\langle \hat{D}_1 \hat{D}_2 \rangle = \int_{\omega_-}^{\omega_+} \frac{e^{-i\tau\Omega} [8G^2\kappa + (\gamma + 2i\Omega)(\kappa^2 + 4\Omega^2)]}{-(\gamma^2 + 4\Omega^2)(\kappa^2 + 4\Omega^2)^2 / (8G^2\kappa)} d\Omega. \quad (13)$$

The effect of time delay τ on entanglement E_n can be seen easily from the equivalent two-mode squeezing thermal state. From Eq. (7), we can see that the two-mode squeezing parameters \bar{n}_1 , \bar{n}_2 , and R_{12} are affected by time delay τ just through the correlator $\langle \hat{D}_1 \hat{D}_2 \rangle$. More specifically, \bar{n}_1, \bar{n}_2 will decrease and R_{12} will increase if the modulus $|\langle \hat{D}_1 \hat{D}_2 \rangle|$ becomes large as other parameters are fixed except for time delay τ . Hence, it is certain that the output entanglement E_n will increase with the increasing of the modulus of the correlator $\langle \hat{D}_1 \hat{D}_2 \rangle$. The optimal time delay τ_{opt} is the delay which makes the $|\langle \hat{D}_1 \hat{D}_2 \rangle|$ reach a maximum. After obtaining the approximate analytical expression about $|\langle \hat{D}_1 \hat{D}_2 \rangle|$ and making some corrections, we find the optimal time delay is

$$\tau_{\text{opt}} \approx \begin{cases} \frac{3G^2\kappa(\omega^2 - \frac{\kappa^2}{8})}{G^4\kappa^2 + \omega^6}, & \omega \geq \frac{\kappa}{2} \\ \frac{\pi\kappa}{2(2+\pi)G^2}, & 0 \leq \omega < \frac{\kappa}{2}. \end{cases} \quad (14)$$

We plot the output entanglement E_n with optimal time delay τ (red solid line) based on Eq. (14), that with numerical optimal time delay (blue dashed line) which makes the entanglement E_n reach a maximum in Fig. 4(a), and the corresponding time delays in Fig. 4(b) with the parameters $\gamma = 1$, $\sigma = \kappa = 10^5$, $G = 10\kappa$, and they all fit very well. It can be seen from Fig. 4(a) that the time delay τ strongly affects the entanglement E_n as long as the center frequency ω is not big enough compared with bandwidth σ , while it has no effect on the entanglement E_n as $\omega \gg \sigma$. The reason is that the effect of increasing ω while fixing σ is equivalent to that of decreasing σ while fixing ω . The time delay τ has no effect on entanglement for the case of $\sigma \rightarrow 0$. It can be seen according to Eq. (13) in which the factor $e^{-i\tau\Omega}$ can be extracted out of the integration for small bandwidth σ with the result that the modulus $|\langle \hat{D}_1 \hat{D}_2 \rangle|$ will be not related to τ . Hence, in the case of $\sigma \rightarrow 0$, the time scale τ_i for the filtered output fields in Eq. (4) can be freely chosen. Finally, the output entanglement becomes steep in the vicinity $\omega = \sigma/2$ because of the special rectangle filter, and takes a local minimum ($E_{n\text{min}} \approx 1.68$) at $\omega = \sigma/2$ according to the numerical result [see the blue dashed line in Fig. 4(a)].

IV. CONCLUSIONS

In summary, we have studied theoretically the output entanglement between two output cavity fields via reservoir engineering by shifting the center frequency of the causal filter function away from the resonance ($\omega = 0$ in the rotating frame) in a three-mode cavity optomechanical system. We find that the nonzero bandwidth σ can largely suppress the entanglement E_n , specifically $E_n \sim 1/\sigma$ in the vicinity of resonant frequency; whereas, the output entanglement will become strong if the filter center frequency departs from the resonant frequency. This is because shifting the filter center frequency can effectively cool the two-mode squeezing thermal state which is equivalent to our model. We obtain

all the approximate analytical expressions of the output entanglement, from which we give the corresponding optimal center frequencies ω_{opt} . In addition, we find the time delay τ between the two output optical fields can evidently affect the output entanglement. And we obtain the analytical expression of the optimal time delay τ_{opt} in the case of large filter bandwidth ($\sigma = \kappa$). Our results can also be applied to other parametrically coupled three-mode bosonic systems, and may be useful to experimentalists to obtain large entanglement.

ACKNOWLEDGMENTS

X.B.Y. is supported by China Postdoctoral Science Foundation (Grant No. 2015M571136).

APPENDIX A: SCATTERING MATRIX

We can solve the Heisenberg-Langevin equations in Fourier space. We define the Fourier transform of operators by $\hat{A}(t) = \frac{1}{\sqrt{2}} \int e^{-i\omega t} \hat{A}(\omega) d\omega$ and $\hat{A}^\dagger(t) = \frac{1}{\sqrt{2}} \int e^{-i\omega t} \hat{A}^\dagger(-\omega) d\omega$. The frequency-resolved output modes $\hat{d}_i^{\text{out}}(\omega) \equiv \int d\omega e^{i\omega t} \hat{d}_i^{\text{out}}(t) / \sqrt{2\pi}$ can be obtained via Fourier transform of operators $\hat{d}_1(t), \hat{d}_2(t), \hat{b}(t)$ and the conjugate operators $\hat{b}^\dagger(t), \hat{d}_1^\dagger(t), \hat{d}_2^\dagger(t)$, and the standard input-output relations $\hat{d}_i^{\text{out}}(t) = \hat{d}_i^{\text{in}}(t) + \sqrt{\kappa_i} \hat{d}_i(t)$ ($i = 1, 2$). For convenience, we define the vectors $v_{\text{out/in}}(\omega) = (d_1^{\text{out/in}}, d_2^{\text{out/in}}, b^{\text{out/in}}, b^{\text{out/in}\dagger}, d_2^{\text{out/in}\dagger}, d_1^{\text{out/in}\dagger})^T(\omega)$.

After a straightforward calculation the solution for the output fields can be written as $v_{\text{out}}(\omega) = S(\omega)v_{\text{in}}(\omega)$ with the scattering matrix $S(\omega)$,

$$S(\omega) = \Gamma M^{-1} \Gamma + I, \quad (A1)$$

where Γ is a diagonal matrix with diagonal element $\Gamma_{jj} = (\sqrt{\kappa_1}, \sqrt{\kappa_2}, \sqrt{\gamma}, \sqrt{\gamma}, \sqrt{\kappa_2}, \sqrt{\kappa_1})$, and

$$M = \begin{pmatrix} m_1 & 0 & -iG_1 & 0 & 0 & 0 \\ 0 & m_2 & 0 & -iG_2 & 0 & 0 \\ -iG_1 & 0 & m_3 & 0 & -iG_2 & 0 \\ 0 & iG_2 & 0 & m_3 & 0 & iG_1 \\ 0 & 0 & iG_2 & 0 & m_2 & 0 \\ 0 & 0 & 0 & iG_1 & 0 & m_1 \end{pmatrix}. \quad (A2)$$

Here, $m_j = i\omega - \frac{\kappa_j}{2}$ ($j = 1, 2, 3$, and κ_3 denotes the mechanical decay rate γ).

APPENDIX B: DEFINITION OF THE LOGARITHMIC NEGATIVITY

Here, we review the definition of the logarithmic negativity and apply it to quantify the entanglement of the filtered optical output fields that can be described as

$$\hat{D}_i^{\text{out}}[\omega, \sigma, \tau_i] = \int d\omega' e^{-i\omega'\tau_i} f(\omega') \hat{d}_i^{\text{out}}(\omega'). \quad (B1)$$

For simplicity, we consider a square filter function centered at ω with bandwidth σ , i.e.,

$$f(\omega') = \frac{\theta[\omega' - (\omega - \frac{\sigma}{2})] - \theta[\omega' - (\omega + \frac{\sigma}{2})]}{\sqrt{\sigma}} \quad (B2)$$

with $\theta[\omega]$ the Heaviside step function. Hence, the filtered optical output fields can be written as

$$\hat{D}_i^{\text{out}}[\omega, \sigma, \tau_i] = \frac{1}{\sqrt{\sigma}} \int_{\omega_-}^{\omega_+} d\omega' e^{-i\omega' \tau_i} \hat{d}_i^{\text{out}}(\omega') \quad (\text{B3})$$

with $\omega_{\pm} = \omega \pm \frac{\sigma}{2}$.

We can use the logarithmic negativity to characterize the entanglement for the output light beams $\hat{D}_1^{\text{out}}[\omega, \sigma, \tau_1]$ and $\hat{D}_2^{\text{out}}[-\omega, \sigma, \tau_2]$. It can be calculated using the expression

$$\text{En} = \max[0, -\ln 2\eta] \quad (\text{B4})$$

with

$$\eta = \frac{1}{\sqrt{2}} \sqrt{\Sigma - \sqrt{\Sigma^2 - \det V}} \quad (\text{B5})$$

and

$$\Sigma = \det B + \det B' - 2 \det C. \quad (\text{B6})$$

The 4×4 covariance matrix V is defined as $V_{jj'} = \frac{1}{2} \langle \hat{u}_j \hat{u}_{j'} + \hat{u}_j \hat{u}_{j'} \rangle$ with $\hat{u} = \{\hat{x}_1, \hat{p}_1, \hat{x}_2, \hat{p}_2\}^T$. Here, $\hat{x}_i = \frac{\hat{D}_i + \hat{D}_i^\dagger}{\sqrt{2}}$ and $\hat{p}_i = \frac{\hat{D}_i - \hat{D}_i^\dagger}{\sqrt{2}i}$. The matrices B , B' , and C are 2×2 matrices related to the covariance matrix V as

$$V = \begin{pmatrix} B & C \\ C^T & B' \end{pmatrix}. \quad (\text{B7})$$

-
- [1] M. Aspelmeyer, T. J. Kippenberg, and F. Marquardt, *Rev. Mod. Phys.* **86**, 1391 (2014).
- [2] T. J. Kippenberg and K. J. Vahala, *Science* **321**, 1172 (2008).
- [3] F. Marquardt and S. M. Girvin, *Physics* **2**, 40 (2009).
- [4] P. Verlot, A. Tavernarakis, T. Briant, P.-F. Cohadon, and A. Heidmann, *Phys. Rev. Lett.* **104**, 133602 (2010).
- [5] S. Mahajan, T. Kumar, A. B. Bhattacharjee, and ManMohan, *Phys. Rev. A* **87**, 013621 (2013).
- [6] S. Gigan, H. Böhm, M. Paternostro, F. Blaser, G. Langer, J. Hertzberg, K. Schwab, D. Bäuerle, M. Aspelmeyer, and A. Zeilinger, *Nature (London)* **444**, 67 (2006).
- [7] D. Kleckner and D. Bouwmeester, *Nature (London)* **444**, 75 (2006).
- [8] J. D. Thompson, B. M. Zwickl, A. M. Jayich, F. Marquardt, S. M. Girvin, and J. G. E. Harris, *Nature (London)* **452**, 72 (2008).
- [9] S. Gröblacher, K. Hammerer, M. R. Vanner, and M. Aspelmeyer, *Nature (London)* **460**, 724 (2009).
- [10] W. Z. Jia, L. F. Wei, Yong Li, and Yu-Xi Liu, *Phys. Rev. A* **91**, 043843 (2015).
- [11] X. B. Yan, C. L. Cui, K. H. Gu, X. D. Tian, C. B. Fu, and J. H. Wu, *Opt. Express* **22**, 4886 (2014).
- [12] F. Marquardt, J. P. Chen, A. A. Clerk, and S. M. Girvin, *Phys. Rev. Lett.* **99**, 093902 (2007).
- [13] I. Wilson-Rae, N. Nooshi, W. Zwerger, and T. J. Kippenberg, *Phys. Rev. Lett.* **99**, 093901 (2007).
- [14] M. Bhattacharya and P. Meystre, *Phys. Rev. Lett.* **99**, 073601 (2007).
- [15] J. Chan, T. P. Mayer Alegre, A. H. Safavi-Naeini, J. T. Hill, A. Krause, Simon Gröblacher, M. Aspelmeyer, and O. Painter, *Nature (London)* **478**, 89 (2011).
- [16] J. D. Teufel, T. Donner, Dale Li, J. W. Harlow, M. S. Allman, K. Cicak, A. J. Sirois, J. D. Whittaker, K. W. Lehnert, and R. W. Simmonds, *Nature (London)* **475**, 359 (2011).
- [17] B. He, L. Yang, Q. Lin, and M. Xiao, *Phys. Rev. Lett.* **118**, 233604 (2017).
- [18] S. Huang and G. S. Agarwal, *Phys. Rev. A* **80**, 033807 (2009).
- [19] S. Weis, R. Rivière, S. Deléglise, E. Gavartin, O. Arcizet, A. Schliesser, and T. J. Kippenberg, *Science* **330**, 1520 (2010).
- [20] A. H. Safavi-Naeini, T. P. Mayer Alegre, J. Chan, M. Eichenfield, M. Winger, Q. Lin, J. T. Hill, D. E. Chang, and O. Painter, *Nature (London)* **472**, 69 (2011).
- [21] Y. X. Liu, M. Davanco, V. Aksyuk, and K. Srinivasan, *Phys. Rev. Lett.* **110**, 223603 (2013).
- [22] A. Kronwald and F. Marquardt, *Phys. Rev. Lett.* **111**, 133601 (2013).
- [23] P. Kómár, S. D. Bennett, K. Stannigel, S. J. M. Habraken, P. Rabl, P. Zoller, and M. D. Lukin, *Phys. Rev. A* **87**, 013839 (2013).
- [24] M. A. Lemonde, N. Didier, and A. A. Clerk, *Phys. Rev. Lett.* **111**, 053602 (2013).
- [25] K. Børkje, A. Nunnenkamp, J. D. Teufel, and S. M. Girvin, *Phys. Rev. Lett.* **111**, 053603 (2013).
- [26] X. Y. Lü, W. M. Zhang, S. Ashhab, Y. Wu, and F. Nori, *Sci. Rep.* **3**, 2943 (2013).
- [27] L. Tian and H. Wang, *Phys. Rev. A* **82**, 053806 (2010).
- [28] K. Stannigel, P. Rabl, A. S. Sørensen, P. Zoller, and M. D. Lukin, *Phys. Rev. Lett.* **105**, 220501 (2010).
- [29] Y. D. Wang and A. A. Clerk, *Phys. Rev. Lett.* **108**, 153603 (2012).
- [30] Y. D. Wang and A. A. Clerk, *New J. Phys.* **14**, 105010 (2012).
- [31] B. Julsgaard, A. Kozhekin, and E. S. Polzik, *Nature (London)* **413**, 400 (2001).
- [32] H. Krauter, C. A. Muschik, K. Jensen, W. Wasilewski, J. M. Petersen, J. I. Cirac, and E. S. Polzik, *Phys. Rev. Lett.* **107**, 080503 (2011).
- [33] A. J. Berkley, H. Xu, R. C. Ramos, M. A. Gubrud, F. W. Strauch, P. R. Johnson, J. R. Anderson, A. J. Dragt, C. J. Lobb, and F. C. Wellstood, *Science* **300**, 1548 (2003).
- [34] M. Neeley, R. C. Bialczak, M. Lenander, E. Lucero, M. Mariantoni, D. Sank, H. Wang, M. Weides, J. Wenner, Y. Yin, T. Yamamoto, A. N. Cleland, and J. M. Martinis, *Nature (London)* **467**, 570 (2010).
- [35] L. DiCarlo, M. Reed, L. Sun, B. L. Johnson, J. M. Chow, J. M. Gambetta, L. Frunzio, S. M. Girvin, M. H. Devoret, and R. J. Schoelkopf, *Nature (London)* **467**, 574 (2010).
- [36] E. Flurin, N. Roch, F. Mallet, M. H. Devoret, and B. Huard, *Phys. Rev. Lett.* **109**, 183901 (2012).
- [37] M. Bhattacharya, P.-L. Giscard, and P. Meystre, *Phys. Rev. A* **77**, 030303(R) (2008).
- [38] R. X. Chen, L. T. Shen, Z. B. Yang, H. Z. Wu, and S. B. Zheng, *Phys. Rev. A* **89**, 023843 (2014).

- [39] J. Q. Liao, Q. Q. Wu, and F. Nori, *Phys. Rev. A* **89**, 014302 (2014).
- [40] C. J. Yang, J. H. An, W. Yang, and Y. Li, *Phys. Rev. A* **92**, 062311 (2015).
- [41] M. Paternostro, D. Vitali, S. Gigan, M. S. Kim, C. Brukner, J. Eisert, and M. Aspelmeyer, *Phys. Rev. Lett.* **99**, 250401 (2007).
- [42] C. Wipf, T. Corbitt, Y. Chen, and N. Mavalvala, *New J. Phys.* **10**, 095017 (2008).
- [43] C. Genes, A. Mari, P. Tombesi, and D. Vitali, *Phys. Rev. A* **78**, 032316 (2008).
- [44] Sh. Barzanjeh, D. Vitali, P. Tombesi, and G. J. Milburn, *Phys. Rev. A* **84**, 042342 (2011).
- [45] Sh. Barzanjeh, M. Abdi, G. J. Milburn, P. Tombesi, and D. Vitali, *Phys. Rev. Lett.* **109**, 130503 (2012).
- [46] Sh. Barzanjeh, S. Pirandola, and C. Weedbrook, *Phys. Rev. A* **88**, 042331 (2013).
- [47] Y.-D. Wang and A. A. Clerk, *Phys. Rev. Lett.* **110**, 253601 (2013).
- [48] L. Tian, *Phys. Rev. Lett.* **110**, 233602 (2013).
- [49] M. C. Kuzyk, S. J. van Enk, and H. Wang, *Phys. Rev. A* **88**, 062341 (2013).
- [50] Y.-D. Wang, S. Chesi, and A. A. Clerk, *Phys. Rev. A* **91**, 013807 (2015).
- [51] Z. J. Deng, S. J. M. Habraken, and F. Marquardt, *New J. Phys.* **18**, 063022 (2016).
- [52] Z. J. Deng, X. B. Yan, Y. D. Wang, and C. W. Wu, *Phys. Rev. A* **93**, 033842 (2016).
- [53] D. Vitali, S. Gigan, A. Ferreira, H. R. Böhm, P. Tombesi, A. Guerreiro, V. Vedral, A. Zeilinger, and M. Aspelmeyer, *Phys. Rev. Lett.* **98**, 030405 (2007).
- [54] S. G. Hofer, W. Wiczorek, M. Aspelmeyer, and K. Hammerer, *Phys. Rev. A* **84**, 052327 (2011).
- [55] U. Akram, W. Munro, K. Nemoto, and G. J. Milburn, *Phys. Rev. A* **86**, 042306 (2012).
- [56] K. Sinha, S. Y. Lin, and B. L. Hu, *Phys. Rev. A* **92**, 023852 (2015).
- [57] Q. Lin, B. He, L. Yang, and M. Xiao, [arXiv:1704.05445](https://arxiv.org/abs/1704.05445).
- [58] T. A. Palomaki, J. D. Teufel, R. W. Simmonds, and K. W. Lehnert, *Science* **342**, 710 (2013).
- [59] C. Dong, V. Fiore, M. C. Kuzyk, and H. Wang, *Science* **338**, 1609 (2012).
- [60] J. T. Hill, A. H. Safavi-Naeini, J. Chan, and O. Painter, *Nat. Commun.* **3**, 1196 (2012).
- [61] R. Andrews, R. W. Peterson, T. P. Purdy, K. Cicak, R. W. Simmonds, C. A. Regal, and K. W. Lehnert, *Nat. Phys.* **10**, 321 (2014).
- [62] J. F. Poyatos, J. I. Cirac, and P. Zoller, *Phys. Rev. Lett.* **77**, 4728 (1996).
- [63] C. A. Muschik, E. S. Polzik, and J. I. Cirac, *Phys. Rev. A* **83**, 052312 (2011).
- [64] E. X. DeJesus and C. Kaufman, *Phys. Rev. A* **35**, 5288 (1987).
- [65] C. Gardiner and P. Zoller, *Quantum Noise*, 3rd ed. (Springer, New York, 2004).
- [66] G. Vidal and R. F. Werner, *Phys. Rev. A* **65**, 032314 (2002).
- [67] M. B. Plenio, *Phys. Rev. Lett.* **95**, 090503 (2005).